Comparative solution equilibrium and structural studies of half-sandwich ruthenium(II)(η^6-toluene) complexes of picolinate derivatives

Jelena M. Poljarević,[a,b] Tamás G. Gál,[c] Nóra V. May,[c] Gabriella Spengler,[d] Orsolya Dömötör,[a] Aleksandar R. Savić,[b] Sanja Grgurić-Šipka,[b] Éva A. Enyedy[a]*

[a] Department of Inorganic and Analytical Chemistry, University of Szeged, Dóm tér 7. H-6720 Szeged, Hungary

[b] Faculty of Chemistry, University of Belgrade, Studentski trg 12-16, 11000 Belgrade, Serbia

[c] Research Centre for Natural Sciences Hungarian Academy of Sciences, Magyar tudósok körútja 2, H-1117 Budapest, Hungary

[d] Department of Medical Microbiology and Immunobiology, University of Szeged, Dóm tér 10, H-6720 Szeged, Hungary

Keywords: Stability constants; X-ray crystal structures; Half-sandwich complexes; Speciation; Antiproliferative activity

* Corresponding author.

E-mail address: enyedy@chem.u-szeged.hu (É.A. Enyedy).

ABSTRACT

Five Ru(II)(η^6-toluene) complexes formed with 2-picolinic acid and its various derivatives have been synthesized and characterized. X-ray structures of four complexes are also reported. Complex formation processes of $[Ru(II)(\eta^6\text{-toluene})(H_2O)_3]^{2+}$ organometallic cation with the metal-free ligands were studied in aqueous solution in the presence of chloride ions by the combined use of ^{1}H NMR spectroscopy, UV-visible spectrophotometry and pH-potentiometry. Solution stability, chloride ion affinity and lipophilicity of the complexes were characterized together with the in vitro cytotoxic and antiproliferative activity in cancer cell lines being sensitive and resistant to classic chemotherapy and in normal cells as well. Formation of mono complexes such as [Ru(η^6-toluene)(L)(Z)] (L: completely deprotonated ligand; Z = H_2O/Cl^-) with high stability and [Ru(η^6-toluene)(L)(OH)] was found in solution. The pK_a values (8.3-8.7) reflect the formation of low amount of mixed hydroxido species at pH 7.4 at 0.2 M KCl ionic strength. The complexes are fairly hydrophilic and show moderate chloride ion affinity and fast chloride-water exchange processes. The studied complexes exhibit no cytotoxic activity in human cancer cells (IC_{50} > 100 μM), only complexes formed with 2-picolinic acid

(**1**) and its 3-methyl derivative (**2**) represented a moderate antiproliferative effect (IC_{50} = 84.8 (**1**), 79.2 μM (**2**)) on a multidrug resistant (MDR) colon adenocarcinoma cell line revealing considerable MDR selectivity. Complexes **1** and **2** are bound to human serum albumin covalently and relatively slowly with moderate strength at multiple binding sites without ligand cleavage.

1. Introduction

Ruthenium complexes have emerged as attractive alternatives to platinum based compounds such as cisplatin, carboplatin and oxaliplatin which are undoubtedly successful anticancer drugs but have several drawbacks such as serious side-effects and lack of activity (drug resistance) against certain types of cancer. Ruthenium compounds have different physico-chemical and pharmacokinetic properties compared to the platinum drugs, and they have different mechanism of action as well, this is the reason why they are the subject of extensive drug discovery efforts [1-3]. Imidazolium *trans*-[tetrachlorido(DMSO)(imidazole)ruthenate(III)] (NAMI-A) was the first Ru(III) complex reached clinical trials [4], while sodium *trans*-[tetrachloridobis(1*H*-indazole)ruthenate(III)] (NKP-1339, IT-139) is one of the most promising investigational non-Pt drugs in current clinical development. NKP-1339 is active against solid malignancies such as non-small cell lung cancer, colorectal carcinoma and the treatment is accompanied by minor side effects [5,6]. While cisplatin induces DNA damage via adduct formation [7], endoplasmic reticulum stress and reactive oxygen species-related effects were found to be involved in the mechanism of action of NKP-1339 [5,8]. Ru(III) complexes are considered as prodrugs that are activated by reduction and it provides the impetus for the development of various Ru(II) anticancer compounds [5]. It is noteworthy that a novel Ru(II) compound [Ru(4,4'-dimethyl-2,2'-bipyridine)$_2$-(2-(2',2'':5'',2'''-terthiophene)-imidazo[4,5-f][1,10]phenanthroline)]Cl_2 (TLD-1433) has entered a human clinical trial recently as nontoxic photosensitizing agent [9]. Ru(II) is often stabilized in the +2 oxidation state by the coordination of η^6-arene type ligands and there are two main prototypes of Ru(II)-arene complexes [3]: i) RAPTA compounds contain 1,3,5-triaza-7-phosphatricyclo-[3.3.1.1]decane (PTA) such as [Ru(η^6-*p*-cymene)(PTA)Cl_2] (RAPTA-C) possessing significant antimetastatic property and is ready for translation into clinical evaluation [10,11]; ii) RAED complexes bear the bidentate 1,2-ethylenediamine (en) ligand such as [Ru(η^6-biphenyl)(en)Cl]PF_6 (RM175) that has a similar cytotoxic activity to cisplatin [12,13]. In most of the half-sandwich organoruthenium(II) compounds a bidentate ligand with an (O,O), (O,S), (O,N), (N,N) or (N,S) binding mode is coordinated and a chloride ion acts as the leaving group [3,14-16]. Aquation (replacement of the chlorido ligand by a water molecule) facilitates the reaction with biological macromolecules such as proteins or DNA, therefore the strength of the Ru-Cl bond and the rate of its cleavage have a strong impact on the bioactivity of the Ru(II)-arene complexes [17]. Notably, the chemical and pharmacological

properties of the Ru(II)-arene half-sandwich compounds can be fine-tuned by variation of the coordinating ligand, the arene ring and the leaving group [1,3,10]. Although a large number of Ru(II)-arene compounds has been developed and extensively investigated, information about their solution speciation and stability constants is still limited in the literature. Most of the solution equilibrium studies are focused on [Ru(η^6-*p*-cymene)(X,Y)Cl] type complexes [18-24]. For the better understanding of the pharmacokinetic properties and mechanisms of action of these metal complexes, the knowledge of the aqueous chemistry and the most plausible chemical forms in water, especially at physiological pH, is a mandatory prerequisite.

In our previous works we have studied the biological activity of Ru(II)(η^6-*p*-cymene) complexes of various pyridine derivatives [25-28] and moderate-to-low cytotoxicity was found in six tumor cell lines; although the complex of 2-picolinic acid (picH) represents an enhanced antiproliferative activity (*e.g.* IC_{50} = 82 μM in HeLa cells, 36 μM in FemX cells [27]) and antimetastatic effect based on wound migration assay [25]. The solution speciation of Ru(II)(η^6-*p*-cymene) picolinate complexes was also studied by some of us revealing the formation of mono-ligand complexes with high stabilities [23]. Notably, the Os(II) congener of the picolinate complex showed very high *in vitro* cytotoxic activity [29].

As the physico-chemical and biological properties can be modified by the exchange of the arene ring, in this work we have prepared and structurally characterized Ru(II)(η^6-toluene) complexes formed with picH and its 3-methyl (3-Me-picH), 5-bromo (5-Br-picH), 2,4-dicarboxylic (2,4-dipicH_2) and 2,5-dicarboxylic (2,5-dipicH_2) derivatives (Chart 1). In addition to the determination of the solid phase structures of the four complexes by X-ray crystallography, solution speciation of these Ru(II)(η^6-toluene) complexes in water was revealed by pH-potentiometry, ^{1}H NMR spectroscopy and UV-visible (UV-vis) spectrophotometry involving studies on their stability and chloride ion affinity. The antiproliferative and cytotoxic effectiveness of these complexes in multidrug resistant/non-resistant human cancer lines was~~ere~~ also tested. Interactions between human serum albumin and the complexes showing antiproliferative effect were monitored using fluorometry and ultrafiltration.

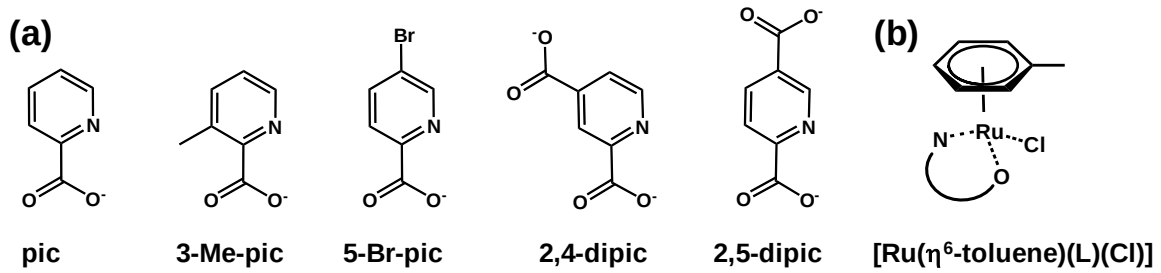

Chart 1. Chemical structures of the ligands in their completely deprotonated forms (a) and the general formula of the prepared [Ru(η^6-toluene)(L)(Cl)] complexes.

2. Experimental

2.1. Chemicals

All solvents were of analytical grade and used without further purification. Pyridine-2-carboxylic acid (2-picolinic acid, picH), 3-methylpyridine-2-carboxylic acid (3-Me-picH), 5-bromo-2-pyridinecarboxylic acid (5-Br-picH), 2,4-pyridinedicarboxylic acid monohydrate (2,4-dipicH_2·H_2O), 2,5-pyridinedicarboxylic acid (2,5-dipicH_2), $RuCl_3$·$3H_2O$, KCl, HCl, KOH, 4,4-dimethyl-4-silapentane-1-sulfonic acid (DSS), 1-methylimidazole (N-MeIm), human serum albumin (HSA, as lyophilized powder with fatty acids, A1653), KH_2PO_4, NaH_2PO_4·$2H_2O$, Na_2HPO_4·$2H_2O$ were purchased from Sigma-Aldrich in *puriss* quality. Doubly distilled Milli-Q water was used for preparation of samples. The purity of the ligands and the exact concentration of their stock solutions were determined by pH-potentiometric titrations and by the computer program HYPERQUAD [30]. [Ru(η^6-toluene)Cl_2]$_2$ was prepared according to a well known procedure [31]. A stock solution of [Ru(η^6-toluene)$(Z)_3$], where Z is H_2O or Cl^-, was obtained by dissolving [Ru(η^6-toluene)Cl_2]$_2$ in water and the exact concentration of this stock was determined with pH-potentiometric titrations. The modified phosphate-buffered saline (PBS') contains 12 mM Na_2HPO_4, 3 mM KH_2PO_4, 1.5 mM KCl and 100.5 mM NaCl; and the concentration of the K^+, Na^+ and Cl^- ions corresponds to that of the human blood serum. HSA solution was freshly prepared before the experiments and its concentration was estimated from its UV absorption: $\varepsilon_{280\,nm}$(HSA) = 36850 $M^{-1}cm^{-1}$ [32]. Stock solution of N-MeIm was prepared on a weight-in-volume basis in PBS' solution.

2.2. Synthesis of the complex [(η^6-toluene)RuCl(μ-Cl)]$_2$ with different picolinic acids

2.2.1. Synthesis of the precursor [Ru(η^6-toluene)Cl(μ-Cl)]$_2$

$[Ru(\eta^6\text{-toluene})Cl(\mu\text{-}Cl)]_2$ was prepared according the literature procedure used for the analogous $[Ru(\eta^6\text{-benzene})Cl(\mu\text{-}Cl)]_2$ [31] by adding 5 mL of 1-methyl-1,4-cyclohexadiene to a solution of 0.5 g $RuCl_3 \cdot 3H_2O$ (1.9 mmol) in 40 mL of absolute ethanol. This mixture was refluxed for 8 h. The reddish brown precipitate formed during the synthesis was filtered off, washed with diethyl ether and left to dry in exsiccator. Yield: 85%, 0.450 g; ^{1}H NMR (500.26 MHz, DMSO-d_6, d, ppm): 2.12 (3H, s, CH_3), 5.68 (3H, m, C2, C4, C6 arene), 5.97 (2H, m, C3, C5 arene); ^{13}C NMR (125.79 MHz MHz, DMSO-d_6) 18.73 (CH_3), 82.22 (C4 arene), 84.83 (C5, C3 arene), 89.28 (C6, C2 arene), 105.82 (C1 arene).

*2.2.2. Synthesis of chlorido[(pyridine-κN-2-carboxylato-κO)(η^6-toluene)ruthenium(II)] (**1**):*

To a warm solution of $[Ru(\eta^6\text{-toluene})Cl_2]_2$ (0.030 g, 0.057 mmol) in 25 mL of 2-propanol, was added a solution of picH (0.015 g, 0.13 mmol) in 2 mL of 2-propanol. The reaction mixture was stirred at room temperature for 7 days and the yellow-range precipitate was formed. Solution was filtered off and product was dried in exsiccator. Yield: 58%, 0.023 g; ^{1}H NMR (500.26 MHz, DMSO-d_6, δ, ppm): 2.15 (3H, s, CH_3), 5.60 (2H, m, C2, C6 arene), 5.70 (1H, m, C4 arene), 5.99 (2H, m, C3, C5 arene), 7.72 (2H, m, C3, C4 ligand), 8.06 (1H, t, C5 ligand), 9.29 (1H, d, C6 ligand); ^{13}C NMR (125.79 MHz, DMSO-d_6) 18.57 (CH_3), 77.07 (C4 arene), 78.44 (C5 arene), 79.71 (C3 arene), 86.15 (C6 arene), 88.06 (C2 arene), 101.01 (C1 arene), 125.31 (C3 ligand), 128.09 (C5 ligand), 139.64 (C4 ligand), 150.89 (C2 ligand), 153.88 (C6 ligand). ESI/MS (m/z): $[M–Cl]^+$ = 315 and $[M–Cl–COO+H^+]^+$ = 272.

*2.2.3. Synthesis of complexes of chlorido[(3-methylpyridine-κN-2-carboxylato-κO)(η^6-toluene)ruthenium(II)] (**2**), chlorido[(5-bromopyridine-κN-2-carboxylato-κO)(η^6-toluene)ruthenium(II)] (**3**), chlorido[(4-carboxylate-pyridine-κN-2-carboxylato-κO)(η^6-toluene)ruthenium(II)] (**4**), chlorido[(5-carboxylate-pyridine-κN-2-carboxylato-κO)(η^6-toluene)ruthenium(II)] (**5**):*

Methanolic solution of the ligand (3-Me-picH (10.4 mg, 0.076 mmol) or 5-Br-picH (15.4 mg, 0.076 mmol) or 2,4-dipic$H_2 \cdot H_2O$ (14.1 mg, 0.076 mmol) or 2,5-dipicH_2 (12.7 mg, 0.076 mmol)) was slowly added in the methanolic (5 mL) solution of $[Ru(\eta^6\text{-}p\text{-toluene})Cl_2]_2$ (20.0 mg, 0.038 mmol) and reaction mixture was stirred for 3 h, at 40°C. Then, reaction volume was reduced to half and desired orange complex was precipitated. Solution was filtered off and product was dried in exsiccator.

2: Yield: 57%, 0.016 g; ^{1}H NMR (500.26 MHz, DMSO-d_6, δ, ppm): 2.16 (3H, s, arene CH_3), 2.54 (3H, s, ligand CH_3), 5.57 (1H, d,C2, arene), 5.60 (1H, d, C6, arene), 5.68 (1H, t, C4 arene), 5.97 (2H, dd, C3, C5 arene), 7.59 (1H, dd, C5 ligand), 7.89 (1H, d, C4 ligand), 9.22 (1H, d, C6 ligand); ^{13}C NMR (125.79 MHz, DMSO-d_6) 18.37 (CH_3, ligand), 18.65 (CH_3, arene), 77.11 (C4 arene), 78.88 (C5 arene), 79.21 (C3 arene), 86.62 (C6 arene), 88.43 (C2 arene), 101.18 (C1 arene), 126.88 (C5 ligand), 137.92 (C4 ligand), 142.70 (C6 ligand), 147.29 (C3 ligand), 152.48 (C2 ligand), 170.89 (COO-Ru). ESI/MS (m/z): $[M–Cl]^+$ = 330 and $[M–Cl–COO+H^+]^+$ = 287.

3: Yield: 52%, 0.017 g; ^{1}H NMR (500.26 MHz, DMSO-d_6, δ, ppm): 2.17 (3H, s, CH_3), 5.63 and 5.67 (2H,dd ,C2, C6 arene), 5.77 (1H, t,C4 arene), 6.06 (2H, m, C3, C5 arene), 7.68 (1H, d, C3 ligand), 8.34 (1H, d, C4 ligand), 9.52 (1H, s, C6 ligand); ^{13}C NMR (125.79 MHz, DMSO-d_6) 18.41 (CH_3), 76.98 (C4 arene), 78.54 (C5 arene), 79.21 (C3 arene), 86.58 (C6 arene), 88.16 (C2 arene), 101.60 (C1 arene), 122.95 (C5 ligand), 126.30 (C3 ligand), 142.28 (C4 ligand), 149.76 (C2 ligand), 154.04 (C6 ligand), 169.69 (COO-Ru). ESI/MS (m/z): $[M–Cl]^+$ = 395 and $[M–Cl–COO+H^+]^+$ = 352.

4: Yield: 56%, 0.017 g; ^{1}H NMR (500.26 MHz, DMSO-d_6, δ, ppm): 2.18 (3H, s, CH_3), 5.66 (2H,dd ,C2, C6 arene),5.75 (1H, t,C4 arene), 6.06 (2H, m, C3, C5 arene), 8.06 (2H, m, C3, C5 ligand), 9.51 (1H, d, C6 ligand), 14.22 (1H, s, free COOH ligand); ^{13}C NMR (125.79 MHz, DMSO-d_6) 18.41 (CH_3), 77.27 (C4 arene), 78.94 (C5 arene), 79.68 (C3 arene), 86.61 (C6 arene), 88.17 (C2 arene), 101.54 (C1 arene), 123.82 (C3 ligand), 126.63 (C5 ligand), 140.93 (C4 ligand), 151.88 (C6 ligand), 155.17 (C2 ligand), 164.66 (COO-Ru), 169.73 (COOH). ESI/MS (m/z): $[M–Cl]^+$ = 360 and $[M–Cl–COO+H^+]^+$ = 317.

5: Yield: 50%, 0.015 g; ^{1}H NMR (500.26 MHz, DMSO-d_6, δ, ppm): 2.18 (3H, s, CH_3), 5.66(1H, d ,C2 arene), 5.70(1H, d, C6 arene),5.80(1H, t, C4 arene), 6.08 (2H, m, C3, C5 arene), 7.89 (1H, d, C4 ligand), 8.51 (1H, d, C3 ligand), 9.56 (1H, s, C6 ligand), 14.20 (1H, s, free COOH ligand); ^{13}C NMR (125.79 MHz, DMSO-d_6) 18.43 (CH_3), 77.11 (C4 arene), 78.72 (C5 arene), 79.32 (C3 arene), 86.53 (C6 arene), 87.99 (C2 arene), 101.46 (C1 arene), 125.29 (C3 ligand), 130.63 (C4 ligand), 140.24 (C5 ligand), 153.28 (C6 ligand), 154.32 (C2 ligand), 164.42 (COO-Ru), 169.56 (COOH). ESI/MS (m/z): $[M–Cl]^+$ = 360 and $[M–Cl–COO+H^+]^+$ = 317.

For the characterization of the prepared complexes ^{1}H and ^{13}C NMR spectroscopy and electrospray ionization mass spectrometry (ESI-MS) were used. NMR spectra were recorded on a Bruker Avance III 500 spectrometer or a Bruker Ultrashield 500 Plus instrument, and DMSO-d_6 was used as solvent. ESI-MS measurements were performed using a Micromass Q-

TOF Premier (Waters MS Technologies) mass spectrometer equipped with electrospray ion source.

2.3. Crystallographic structure determination

Single crystals suitable for X-ray diffraction experiment of compounds [Ru(η^6-toluene)(pic)Cl] (**1**), [Ru(η^6-toluene)(3-Me-pic)Cl]·H_2O (**2**·H_2O), [Ru(η^6-toluene)(5-Br-pic)Cl] (**3**) and [Ru(η^6-toluene)(2,5-dipic)Cl] (**5**) were grown from methanol solution of the solid complexes.

Orange (**1**) and yellow (**2**·H_2O**, 3, 5**) single crystals were mounted on loops and transferred to the goniometer. X-ray diffraction data were collected at –170 °C (for **1**, **2**·H_2O) or 20 °C (for **3**, **5**) on a Rigaku RAXIS-RAPID II diffractometer using Mo-*K*α radiation. A numerical absorption correction [33] was carried out using the program CrystalClear [34]. Sir2014 [35] and SHELXL [36] under WinGX [37] software were used for structure solution and refinement, respectively. The structures were solved by direct methods. The models were refined by full-matrix least squares on F^2. Refinement of non-hydrogen atoms was carried out with anisotropic temperature factors. Hydrogen atoms were placed into geometric positions (except for water hydrogens which were constrained). They were included in structure factor calculations but they were not refined. The isotropic displacement parameters of the hydrogen atoms were approximated from the U(eq) value of the atom they were bonded to. The summary of data collection and refinement parameters are collected in Table S1. Selected bond lengths and angles of compounds were calculated by PLATON software [38]. The graphical representation and the edition of CIF files were done by Mercury [39] and PublCif [40] softwares, respectively. The crystallographic data files for the complexes have been deposited with the Cambridge Crystallographic Database as CCDC x, CCDC x, CCDC x and CCDC x.

2.4. pH-potentiometric measurements and data evaluation

The pH-potentiometric measurements determining the proton dissociation and formation constants were carried out at 25 ± 0.1°C and an ionic strength I = 0.20 M (KCl) in order to keep the activity coefficient constant. The titrations were performed in a carbonate-free KOH solution (0.20 M). The exact concentrations of HCl and KOH were determined by pH-potentiometric titrations. An Orion 710A pH-meter equipped with a Metrohm combined electrode (type 6.0234.100) and Methrom 665 Dosimat burette were used for the pH-potentiometric measurements. The electrode system was calibrated to the pH= – log[H^+] scale by means of black titrations (strong acid HCl *vs.* strong base KOH), as suggested by Irving *et*

al. [41]. The average water ionization constant, $pK_{w,}$ was determined as 13.76 ± 0.01, which corresponds well to the literature data [42]. The reproducibility of the titration points included in the calculations was within 0.005 pH. The pH-potentiometric titrations were performed in the pH range 2.0 to 11.5. The initial volume of the samples was 5 mL. The ligand concentration was 2 mM and metal to ligand ratios of 1:1 and 1:2 were used. The accepted fitting between the measured and calculated titration data points regarding the volume of the titrant was < 10 μL. The samples were degassed by bubbling purified argon through them for 10 min prior the measurements and the argon was also passed over the solutions during the titrations.

The computer program HYPERQUAD [30] was utilized to establish the stoichiometry of the complexes and to calculate the overall stability constants. $\beta(M_pL_qH_r)$ is defined for the general equilibrium:

$$pM + qL + rH \rightleftharpoons M_pL_qH_r \text{ as } \beta(M_pL_qH_r) \rightleftharpoons [M_pL_qH_r]/[M]^p[L]^q[H]^r \quad (1)$$

where M denotes the metal moiety $[Ru(\eta^6\text{-toluene})(Z)_3]$ (Z = H_2O/Cl^-) and L the completely deprotonated ligand. In all calculations exclusively titration data were used from experiments in which no precipitate was visible in the reaction mixture. As equilibrium constants were determined in the presence of 0.2 M chloride ion, they are considered as conditional constants. logβ values for the various hydroxido complexes$[(Ru(\eta^6\text{-toluene}))_2(\mu^2\text{-OH})_i]^{(4-i)+}$ (i=2,3) were calculated based on the pH-potentiometric titration data in the presence of chloride ions and were found to be in fairly good agreement with previously published data [43].

2.5. UV-vis spectrophotometric and ^{1}H NMR spectroscopic titrations, and determination of the distribution coefficients

A Hewlett Packard 8452A diode array spectrophotometer was used to record the UV-vis spectra in the interval 200 – 800 nm. The path length was 1 cm. Equilibrium constants (proton dissociation, stability constants and H_2O/Cl^- exchange constants) and the individual spectra of the species were calculated with the computer program PSEQUAD [44]. The spectrophotometric titrations were performed in pure water on samples containing the ligands with or without the organometallic cation and the concentration of the ligands was 120 μM. The organometallic cation was also titrated (120 μM) separately. The metal-to-ligand ratios were 1:1 in the pH range from 2 to 11.5 at 25.0±0.1 °C at an ionic strength of 0.20 M (KCl). Measurements for 1:1 metal-to-ligand systems were also carried out by preparing individual samples in which KCl was partially or completely replaced by HCl; pH values, varying in the range *ca.*0.7–2.5, were calculated from the strong acid content. The absorbance data were

always recorded after 4 h of incubation. UV-vis spectra recorded as a function of chloride concentrations (0–252 mM) were used to investigate the H_2O/Cl^- exchange processes of complexes [Ru(η^6-toluene)(L)(H_2O)] at pH 7.40 (using 20 mM phosphate buffer).

^{1}H NMR titrations were carried out on a Bruker Ultrashield 500 Plus instrument using WATERGATE water suppression pulse scheme. DSS was used as an internal NMR standard. ^{1}H NMR spectra of samples containing [Ru(II)(η^6-toluene)(H_2O)$_3$]$^{2+}$ (1 mM) and ligand picH (1 mM) in D_2O at various pH values were recorded after 4 h of incubation (25 °C, I = 0.20 M (KCl)). Titration of 2 mM solution of [Ru(η^6-toluene)(Z)$_3$] was also performed separately. To study the interaction with HSA and N-MeIm ^{1}H NMR spectra were recorded for samples containing precursor [Ru(η^6-toluene)Cl(μ-Cl)]$_2$ or complex **1** (1 mM), with or without half equivalent of HSA or N-MeIm. Samples were prepared in PBS′ buffer and incubated for 24 h at 25 °C.

Distribution coefficients at physiological pH ($D_{7.4}$) of the complexes **1**–**5** and the ligands as well as the Ru precursor were determined by the traditional shake-flask method in *n*-octanol/buffered aqueous solution at pH 7.40 at various chloride concentrations using UV-vis detection as described in our former work [24].

2.6. Fluorescence and membrane ultrafiltration/UV-vis studies with HSA

Fluorescence spectra were recorded on a Hitachi-F4500 fluorometer in 1 cm quartz cell at 25.0 ± 0.1 °C. All solutions were prepared in PBS' (pH 7.4) and were incubated for 24 h following a time-dependence experiment. Samples contained 1 μM HSA, and various HSA-to- Ru(η^6-toluene) or **1** or **2** ratios (from 1:0 to 1:10) were used. The excitation wavelength was 295 nm and the emission was read in the range of 310-500 nm. The quenching (K_Q') constants were calculated with the computer program PSEQUAD [44] using the same approach applied in our previous works [45,46].

Samples (0.50 mL) used for the ultrafiltration studies contained 40 μM HSA and Ru(η^6-toluene) or **1** or **2** (up to 1:10 protein-to-complex ratio) in PBS' buffer (pH 7.4) at 25.0 ± 0.1 °C and were incubated for 24 h. Samples were separated by ultrafiltration through 10 kDa membrane filters (Millipore Amicon Ultra-0.5 centrifugal filter unit) in low (LMM) and high molecular mass (HMM) fractions with the help of a temperature controlled centrifuge (Sanyo, 10000 rpm, 10 min). The LMM fraction containing the non-bound metal complex was separated from the protein and its adducts in the HMM fraction. The concentration of the non-bound

compounds in the LMM fractions was determined by UV-vis spectrophotometry by comparing the recorded spectra to those of reference samples without the protein.

2.7. Cell lines

Human colonic adenocarcinoma cell lines Colo 205 doxorubicin-sensitive (ATCC-CCL-222) and Colo 320/MDR-LRP multidrug resistant overexpressing ABCB1 (MDR1)-LRP (ATCC-CCL-220.1) were purchased from LGC Promochem, Teddington, UK. The cells were cultured in RPMI 1640 medium supplemented with 10% heat-inactivated fetal bovine serum, 2 mM L-glutamine, 1 mM sodium pyruvate and 100 mM 4-(2-hydroxyethyl)-1-piperazineethanesulfonic acid (HEPES). The cell lines were incubated at 37 °C, in a 5% CO_2, 95% air atmosphere. The semi-adherent human colon cancer cells were detached with Trypsin-Versene (EDTA) solution for 5 min at 37 °C.

MRC-5 human embryonal lung fibroblast cell line~~s~~ (ATCC CCL-171) was~~ere~~ purchased from LGC Promochem, Teddington, UK. The cell line was cultured in Eagle's Minimal Essential Medium (EMEM, containing 4.5 g/L glucose) supplemented with a non-essential amino acid mixture, a selection of vitamins and 10% heat-inactivated fetal bovine serum. The cell ~~line~~s were incubated at 37 °C, in a 5% CO_2, 95% air atmosphere.

2.8. Assay for cytotoxic effect

In the study MRC-5 non-cancerous human embryonic lung fibroblast and human colonic adenocarcinoma cell lines (doxorubicin-sensitive Colo 205 and multidrug resistant Colo 320 colonic adenocarcinoma cells) were used to determine the effect of compounds on cell growth. The effects of increasing concentrations of compounds (complexes **1**-**5**, the metal-free ligands, the precursor $[Ru(\eta^6\text{-toluene})Cl(\mu\text{-}Cl)]_2$ and *cis*-$[Pt(NH_3)_2(Cl)_2]$, and the positive control (~~(~~cisplatin (~~,~~ Teva)) on cell growth were tested in 96-well flat-bottomed microtiter plates. The compounds were diluted in a volume of 100 µL of medium.

The adherent human embryonal lung fibroblast cells were cultured in 96-well flat-bottomed microtiter plates, using EMEM supplemented with 10% heat-inactivated fetal bovine serum. The density of the cells was adjusted to 2×10^4 cells in 100 µL per well, the cells were seeded for 24 h at 37 °C, 5% CO_2, then the medium was removed from the plates containing the cells, and the dilutions of compounds previously made in a separate plate were added to the cells in 200 µL.

In case of the colonic adenocarcinoma cells, the two-fold serial dilutions of compounds were prepared in 100 µL of RPMI 1640, horizontally. The semi-adherent colonic

adenocarcinoma cells were treated with Trypsin-Versene (EDTA) solution. They were adjusted to a density of 2×10^4 cells in 100 μL of RPMI 1640 medium, and were added to each well, with the exception of the medium control wells. The final volume of the wells containing compounds and cells was 200 μL.

The culture plates were incubated at 37 °C for 24 h; at the end of the incubation period, 20 μL of MTT (thiazolyl blue tetrazolium bromide, Sigma-Aldrich) solution (from a stock solution of 5 mg/mL) were added to each well. After incubation at 37 ˚C for 4 h, 100 μL of sodium dodecyl sulphate (SDS) (Sigma-Aldrich) solution (10% in 0.01 M HCI) were added to each well and the plates were further incubated at 37 °C overnight. Cell growth was determined by measuring the optical density (OD) at 540/630 nm with Multiscan EX ELISA reader (Thermo Labsystems, Cheshire, WA, USA). Inhibition of the cell growth was determined according to the formula below:

$$IC_{50} = 100 - \left[\frac{OD\,sample - OD\,medium\,control}{OD\,cell\,control - OD\,medium\,control} \right] \times 100$$

Results are expressed in terms of IC_{50}, defined as the inhibitory dose that reduces the growth of the cells exposed to the tested compounds by 50%.

2.9. Assay for antiproliferative effect

The method is similar to the one described in the assay described in Section 2.8 and antiproliferative effect of complexes **1**-**5**, the metal-free ligands, the precursor $[Ru(\eta^6\text{-toluene})Cl(\mu\text{-}Cl)]_2$ and cisplatin was determined. In the assay testing the inhibition of cell proliferation, 6×10^3 colon adenocarcinoma cells were distributed in 100 μL of medium with the exception of the medium control wells. The culture plates were incubated at 37 °C for 72 h and after the incubation time the plates were stained with MTT according to the experimental protocol applied for the cytotoxicity assay *vide supra*.

3. Results and discussion

3.1. Synthesis, characterization and X-ray diffraction analysis of organometallic Ru(II) complexes

The Ru(II) precursor $[Ru(\eta^6\text{-toluene})Cl(\mu\text{-}Cl)]_2$ and the complexes of picH, 3-Me-picH, 5-Br-picH, 2,4-dipicH_2 and 2,5-dipicH_2 (Chart 1) were obtained according to the literature procedure used for the analogous $[Ru(\eta^6\text{-}p\text{-cymene})$ complexes [25-28]. Pure compounds (**1**-**5**) were

isolated from methanol or 2-propanol with moderate yields 50-58%. The organometallic Ru(II) complexes were characterized by means of standard analytical methods (^{1}H , ^{13}C NMR and ESI-MS). The ^{1}H NMR spectra of complexes confirm the coordination of the ligands manifesting itself in downfield or upfield shifts of the pyridine protons (*e.g.* in the case of **1** the C3, C4 protons of the ligand are upfield while C5, C6 are downfield shifted upon coordination as shown in Fig. S1). Similar observations were made for the analogous Ru(II)(η^6-*p*-cymene) complex of picH [27]. In general, signals representing protons next to the pyridine nitrogen were shifted distinctly upon coordination.

Single crystals of complexes **1**, **2**·H_2O, **3** and **5** were obtained by the slow diffusion method from methanol and their structures were determined by single crystal X-ray diffraction. The ORTEP representations of these complexes are depicted in Fig. 1. The complexes **1** and **2**·H_2O crystallized in monoclinic crystal systems in space group $P2_1/n$ and $P2_1$, respectively.

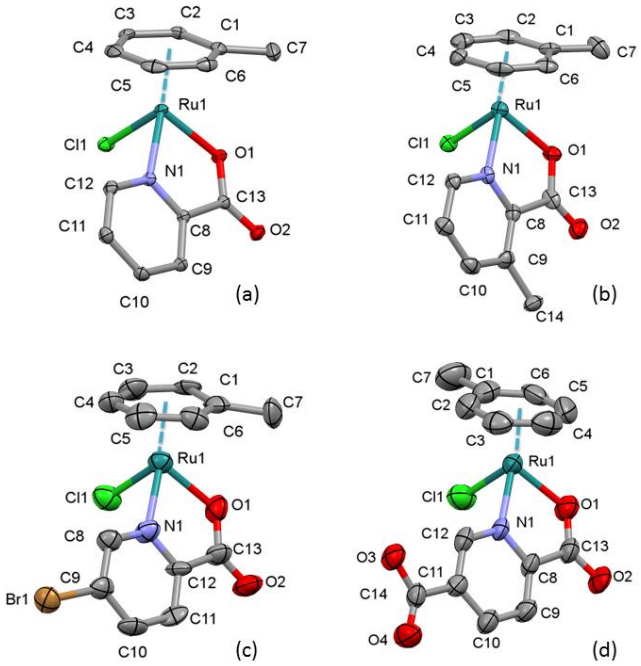

Figure 1. Molecular structures of ruthenium complexes in crystal **1** (a) in crystal **2** (b) in crystal **3** and (c) in crystal **5** (d). Displacement parameters are drawn at 50% probability level; hydrogen atoms and water molecule for **2** are omitted for clarity.

The crystals **3** and **5** crystallized in triclinic crystal systems in space group *P*-1. All of the complexes adopt the so-called "piano stool" configuration, whereby toluene forms the seat and the chelating picolinate ligand as well as the chlorido leaving group constitute the chair legs. In these half-sandwich complexes the ligand is coordinated through the pyridine nitrogen and the carboxylate oxygen. In these structures Ru(II) is a chiral centre. In crystals **1**, **3** and **5** both

enantiomers were crystallized in non-chiral space groups. On the other hand complex **2** crystallized together with a solvate water molecule and only one enantiomer could be found in the chiral space group $P2_1$. The absolute configuration R_{Ru} could be determined according to CIP convention [47], the Flack parameter is 0.01(5). The molecular structures of the studied complexes were directly compared to that of the benzene derivative [Ru(η^6-C_6H_6)(pic)(Cl)] defined previously (Ref code OHUFUT [48]) which crystallized without solvate inclusion in triclinic *P*-1 space group (Fig. 2.) Selected bond distances and angles are collected in Table 1 for comparison. Distances between the toluene ring and the Ru ion are within the range of observed other ruthenium arene half-sandwich complexes (2.079(11)-2.392(7) Å) [49]. Bond lengths and angles do not show significant differences compared to each other (Table 1).

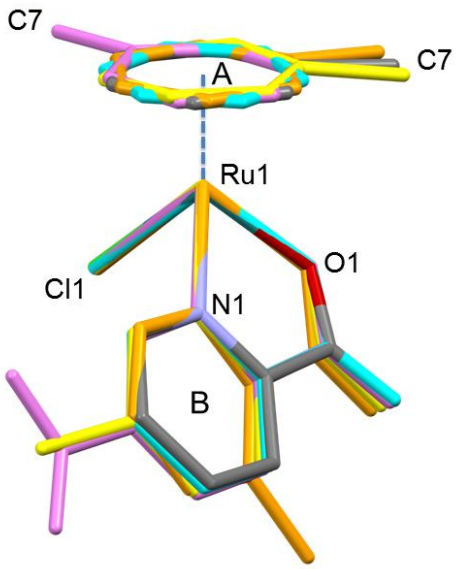

Figure 2. Comparison of molecular structures of Ru(II)(η^6-toluene) picolinate complexes **1** (colored by element), **2** (orange), **3** (yellow), **5** (violet) together with [Ru(η^6-C_6H_6)(pic)(Cl)] (CSD Ref. code OHUFUT) (cyan) [48]. Atoms Ru1, Cl1, N1 and O1 are superimposed.

However, the angles between planes of CgA and CgB (where Cg is the centre of gravity calculated for rings A and B, respectively) show slight differences (Table 1 and Fig. 2). The methyl groups of the toluene molecule are almost in the same position for crystals **1**, **2**·H_2O and **3** (the torsion angle O1-Ru1-Cg(A)-C7 is 5.5 °, 13.3° and -7.7° degree for **1**, **2**·H_2O and **3**, respectively). However, there is a significant difference in crystal **5** where the methyl group turns to the side of the chloride ion and this torsion angle is 116.2°).

Table 1. Selected bond distances (Å) and angles (°) of the studied Ru(II)(η^6-toluene) picolinate complexes in crystals **1-3, 5** and [Ru(η^6-C_6H_6)(pic)(Cl)] (OHUFUT [48])

	1	**2**·H_2O	**3**	**5**	OHUFUT
Bond length (Å)					
Ru1-Cl1	2.4133(5)	2.415(2)	2.405(4)	2.396(3)	2.4133(6)
Ru1-O1	2.074(1)	2.063(6)	2.085(9)	2.093(6)	2.075(2)
Ru1-N1	2.089(2)	2.092(8)	2.11(1)	2.095(7)	2.087(2)
Ru1-C1	2.183(2)	2.179(9)	2.17(1)	2.21(1)	2.178(3)
Ru1-C2	2.194(2)	2.18(1)	2.23(1)	2.17(1)	2.179(3)
Ru1-C3	2.185(2)	2.18(1)	2.16(1)	2.14(1)	2.191(3)
Ru1-C4	2.187(2)	2.17(1)	2.16(1)	2.16(1)	2.190(3)
Ru1-C5	2.148(2)	2.159(8)	2.21(1)	2.14(1)	2.168(3)
Ru1-C6	2.174(2)	2.172(9)	2.16(1)	2.16(1)	2.160(3)
Ru1-Cg(A)[a]	1.6564(9)	1.656(4)	1.662(6)	1.659(5)	1.662
Bond angles (°)					
O1-Ru1-N1	77.04(6)	76.8(3)	77.0(4)	77.4(3)	77.54(9)
O1-Ru1-Cl1	87.44(4)	84.9(2)	85.9(3)	87.0(2)	87.04(6)
N1-Ru1-Cl1	85.73(4)	83.7(2)	83.6(3)	84.2(2)	84.20(7)
Cg(A)-Ru1-O1 [a]	127.69(5)	129.3(2)	129.6(4)	128.4(3)	128.77
Cg(A)-Ru1-N1 [a]	132.73(5)	133.6(2)	134.2(4)	132.8(3)	132.55
Cg(A)-Ru1-Cl1 [a]	128.74(4)	129.66(17)	128.2(2)	129.1(2)	128.97
Cg(A)-Cg(B)[b]	52.94(9)	64.1(5)	61.9(7)	58.9(6)	55.30
O1-Ru1-Cg(A)-Cl1	5.5	13.3	-7.8	116.2	-

[a] Cg is the centre of gravity calculated for ring A. [b] Angles between planes calculated for rings A and B.

The positions of the picolinate ligands are slightly different in the studied complexes due to secondary interactions with adjacent molecules as different molecular arrangements and solvate inclusion (for crystal **2**·H_2O) realized in these crystal structures. The packing arrangements are shown in Figs. S2-S4 viewing along selected crystallographic axes. The main secondary interactions between molecules are C-H…O hydrogen bonds between the toluene hydrogens and the carboxylate oxygen (O1) of the picolinate ligand. Beside the hydrogen bonds considerable secondary interactions are formed between neighboring complexes by C-H…Cl interactions (*e.g.* C12-H12…Cl1 in **2**·H_2O and C5-H5…Cl1 in **4,** Table S2 and Figs. S3 and S5).

3.2. Proton dissociation processes of the studied ligands and hydrolysis of [Ru(η^6-toluene)$(H_2O)_3]^{2+}$ organometallic cation

Proton dissociation constants of the ligands picH, 3-Me-picH, 5-Br-picH, 2,4-dipicH_2 and 2,5-dipicH_2 (Chart 1) were determined by pH-potentiometric and UV-vis spectrophotometric titrations performed in the pH range from 2 up to 11.5 (Table 2). Molar absorbance spectra of the ligand species in the different protonation states were calculated via the deconvolution of the spectra recorded at various pH values as it is shown in Fig. S6 for 5-Br-picH. The pK_a value picH and the calculated molar absorbance spectra of the HL and L^- forms are in reasonably good agreement with data reported previously [23,50]. The protonated compounds picH, 3-Me-picH, 5-Br-picH possess two, while 2,4-dipicH_2 and 2,5-dipicH_2 have three dissociable protons. It was found in all cases that the first deprotonation step assigned to the carboxylic group at position 2 takes place in a fairly acidic range and no pK_a values could be determined for this process. Therefore this carboxylate remains deprotonated in the whole studied pH range. pK_a determined for picH, 3-Me-picH, 5-Br-picH can be attributed to the deprotonation of the pyridinium (NH^+) group as well as the higher pK_a of 2,4-dipicH_2 and 2,5-dipicH_2. The lower pK_a of the latter two ligands belongs to the carboxylic group at position 4 and 5, respectively. Comparing the pK_a values to that of Hpic, it is worth mentioning that the methyl substituent has no measurable effect at position 3, while the bromo and the carboxylic groups decrease the pK_a (NH^+) significantly due to the electron withdrawing power of the halogen substituent and the mesomeric effect of the COO^- moiety.

Based on the determined pK_a values it can be declared that all the studied ligands are present in their completely deprotonated forms (L^-: pic, 3-Me-pic, 5-Br-pic; L^{2-}: 2,4-dipic, 2,5-dipic) at pH 7.4 resulting in their strongly hydrophilic character (log$D_{7.4} < -2$).

Table 2. Proton dissociation constants (pK_a) of the studied ligands determined by pH-potentiometric and UV-vis spectrophotometric titrations; λ_{max} and molar absorptivity (ε) values for the ligand species in the different protonation states. {T = 25.0°C, I = 0.20 M (KCl)}

	Method	**pK_a** (COOH)	**pK_a** (NH^+)	**λ_{max}** (nm) / **ε** ($M^{-1}cm^{-1}$)
pic	pH-metry	< 1	5.13 ±0.03	HL: 263 / 7100
	UV-vis	< 1	5.07 ±0.01	L^-: 263 / 3900
3-Me-pic	pH-metry	< 1	5.16 ±0.03	HL: 274 / 6820
	UV-vis	< 1	5.16 ±0.03	L^-: 268 / 4400

5-Br-pic	pH-metry	< 1	3.44 ±0.02	HL: 278 / 6570; 240 / 9770
	UV-vis	< 1	3.34 ±0.04	L^-: 268 / 4400; 232 / 10650
2,4-dipic	pH-metry	1.84 ±0.05	4.70 ±0.02	H_2L: 278 / 5100
	UV-vis	1.9 ±0.1	4.56 ±0.08	HL^-: 274 / 5980
				L^{2-}: 276 / 3700
2,5-dipic	pH-metry	2.19 ±0.05	4.63 ±0.04	H_2L: 272 / 6900
	UV-vis	2.16 ±0.02	4.57 ±0.01	HL^-: 272 / 7100
				L^{2-}: 272 / 5500

Hydrolytic behavior of the organometallic cation $[Ru(\eta^6\text{-toluene})(H_2O)_3]^{2+}$ has been already studied by Buglyó *et al.* in the presence and in the absence of chloride ions [43]. In the latter case the fast hydrolysis of the aquated organoruthenium cation yields the species $[(Ru(\eta^6\text{-toluene}))_2(\mu^2\text{-}OH)_3]^+$ that becomes predominant at pH > 5. When 0.2 M KCl was used as the background electrolyte, as in our studies, formation of various chlorido and mixed chlorido/hydroxido species as intermediates was found in addition to the major hydrolysis product $[(Ru(\eta^6\text{-toluene}))_2(\mu^2\text{-}OH)_3]^+$. In a good accordance with their findings based on the combined use of ^{1}H NMR spectroscopy and ESI-MS, we have also detected three different species based on the ^{1}H NMR spectra recorded at various pH values (Fig. S7). Namely, the identified species are $[Ru(\eta^6\text{-toluene})(H_2O)_2Cl]^+$ (= M), $[(Ru(\eta^6\text{-toluene}))_2(\mu^2\text{-}OH)_2Cl]^+$ (= $[M_2(OH)_2]$) and $[(Ru(\eta^6\text{-toluene}))_2(\mu^2\text{-}OH)_3]^+$ (= $[M_2(OH)_3]^+$). Overall stability constants for the dinuclear hydrolysis products $[(Ru(\eta^6\text{-toluene}))_2(\mu^2\text{-}OH)_i]^{(4-i)+}$ (i=2,3) were determined by pH-potentiometric and UV-vis spectrophotometric titrations at 0.2 M chloride ion concentration (Table 3) and are in good agreement with data obtained by Buglyó *et al.* using pH-potentiometry [43]. Notably these are conditional stability constants being valid only at 0.2 M KCl ionic strength. Concentration distribution curves were computed on the basis of the stability constants determined by pH-potentiometry showing that the hydrolysis is suppressed somewhat due to the presence of chloride ions, since $[M_2(OH)_3]$ dominates only at pH > 6 (Fig. S8). The ^{1}H NMR signals of the three kinds of species (M, $[M_2(OH)_2]$, $[M_2(OH)_3]$) could be integrated and distribution of the organometallic fragment was calculated showing an acceptable match between the two kinds of methods.

3.3. Complex formation equilibria of [Ru(η^6-toluene)(H_2O)$_3$]$^{2+}$ with the picolinate ligands: stability, deprotonation, chloride ion affinity and lipophilicity

Complexation processes were studied by the combined use of pH-potentiometric, UV-vis spectrophotometric titrations and ^{1}H NMR spectroscopy in a 0.2 M chloride-containing medium. Therefore the formation (log*K* [ML]) and deprotonation (pK_a [ML]) constants determined herein are considered as conditional stability constants. The complex formation between [Ru(η^6-toluene)(H_2O)$_3$]$^{2+}$ and the studied bidentate picolinate ligands follows a fairly simple scheme (Chart S1). Namely a mono complex [Ru(η^6-toluene)(L)(Z)] (=[ML]) is formed, and a mixed hydroxido species [ML(OH)] appears by the deprotonation of the coordinated H_2O molecule and/or by the displacement of the chlorido co-ligand by OH^- in the basic pH range, similarly to the behavior of analogous half-sandwich Ru(η^6-*p*-cymene) complexes [22,23]. The complex formation of the organometallic cation with the picolinate ligands was found to be a rather slow process. *E.g.* the steady state could be reached after more than 35 min in the [Ru(η^6-toluene)(H_2O)$_3$]$^{2+}$ – picH system at pH 2.8 as the time-dependence of the UV-vis spectra indicates (Fig. 3). This slow reaction hindered the application of conventional pH-potentiometric titrations to determine the log*K* [ML] values. In order to solve this problem, individual samples were prepared by the addition of different amount of strong base under argon, and the UV-vis spectra and the actual pH values were measured after 4 h. Based on the recorded spectra it could be concluded that the complex formation proceeds in a great extent already at pH 2 in all cases. As a consequence log*K* [ML] constants were determined from the UV-vis spectral changes of the metal-to-ligand charge-transfer (Ru $4d^6 \rightarrow \pi^*$) and ligand ($\pi \rightarrow \pi^*$) transition bands in the pH range from 0.7 to 3.0 in the case of 3-Me-pic and 2,4-dipic (Table 2). On the other hand, the spectra were unchanged from pH 3 down to pH 0.7 in the [Ru(η^6-toluene)(H_2O)$_3$]$^{2+}$ – pic/5-Br-pic/2,5-dipic systems showing negligible decomposition of the complexes under such strongly acidic conditions. Thus for the log*K* [ML] constants only a lower limit could be estimated (Table 3). Based on these findings the complexation of pic with [Ru(η^6-*p*-cymene)(H_2O)$_3$]$^{2+}$ was reinvestigated using longer incubation times (4 h) needed to reach steady state in the presence of chloride ions (0.2 M KCl) and a higher log*K* [ML] value (>11.5) was obtained than previously published [23].

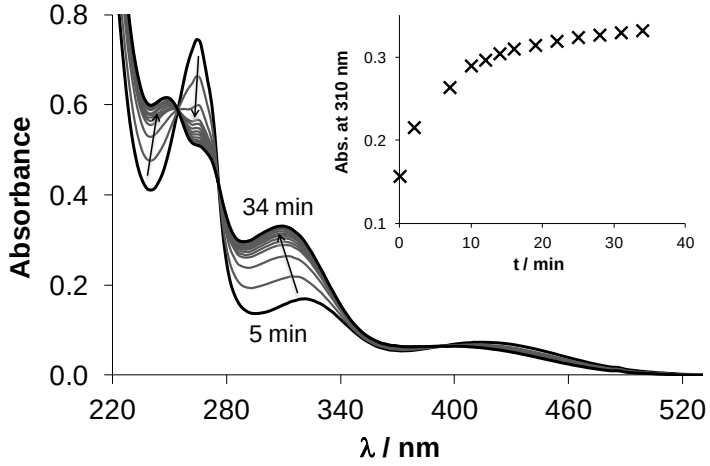

Figure 3. Time-dependence of UV-vis absorption spectra recorded for the $[Ru(\eta^6\text{-toluene})(H_2O)_3]^{2+}$ – picH (1:1) system in the presence of chloride ions. The inset shows the absorbance changes at 310 nm. {c_{Ru} *= 102 μM; T = 25 ˚C; I = 0.20 M (KCl); ℓ = 1.0 cm*}.

Table 3. Stability constants log*K* [ML], pK_a [ML] values of the $[Ru(\eta^6\text{-toluene})(H_2O)_3]^{2+}$ complexes formed with picolinate ligands in 0.2 M chloride-containing aqueous solutions determined by various methods; H_2O/Cl^- exchange constants (log*K*') for the $[Ru(\eta^6\text{-toluene})(L)(H_2O)]^+$ complexes and pM* values at pH = 7.4 (pM* = −log([M] + $[M_2(OH)_3]$ + $[M_2(OH)_2]$) at c_M = 100 μM). {T = 25.0 ˚C, I = 0.20 M (KCl)}

		log*K* [ML]	**p*K*$_a$ [ML]**	**p*K*$_a$ [ML]**	**pM***	**log*K*' (H_2O/Cl^-)**
ligand	complex	UV-vis	UV-vis	pH-metry		UV-vis
pic	**1**	>10.6 [a]	8.53 ±0.01 [b]	8.47 ±0.01 [b]	>5.8	1.33 ±0.01
3-Me-pic	**2**	9.87 ±0.01	8.71 ±0.01	8.68 ±0.05	5.3	1.32 ±0.01
5-Br-pic	**3**	> 8.9 [a]	8.47 ±0.01	8.41 ±0.03	>4.7	1.50 ±0.01
2,4-dipic	**4**	11.22 ±0.07	8.44 ±0.01	8.37 ±0.06	6.2	1.23 ±0.01
2,5-dipic	**5**	> 11.9 [a]	8.58 ±0.01	8.38 ±0.07	>6.7	1.09 ±0.01

[a] Estimated values based on UV-vis spectrum recorded at pH 0.7; [b] pK_a [ML] values based on ^{1}H NMR titrations: 8.52 ±0.09 (0.2 M KCl) and 7.87 ±0.09 (0 M KCl)

Increasing the pH values the studied [ML] complexes may undergo a combination of deprotonation and decomposition. Deprotonation of the coordinated water molecule (and/or $Cl^- \rightarrow OH^-$ exchange) results in the formation of mixed hydroxido [ML(OH)] complexes, while decomposition can yield unbound ligand and metal ion in hydrolyzed forms depending on the actual pH. The recorded UV-vis spectra were the same in a wide pH range (*e.g.* in the $[Ru(\eta^6\text{-}$

toluene)$(H_2O)_3]^{2+}$ – 3-Me-picH system at pH between 3.1 and 7.6 shown in Fig. 4), while significant spectral changes are observed at pH > 8 due to the formation of [ML(OH)]. The appearance of isosbestic points suggests that the metal complexes do not decompose under these conditions; merely they are deprotonated almost in all cases. It should be noted that the complex of 5-Br-pic showed a low extent of decomposition in the basic pH-range. Based on these spectral changes pK_a [ML] constants were determined for the complexes (Table 3). Notably, the spectra of the complexes did not change over a 24 h period at both pH 7.4 and 11 values, and the deprotonation process was found to be rather fast. Therefore pH-potentiometric titrations were also performed to determine pK_a [ML] constants (Table 3) started from pH ~4 but only after a 4 h waiting period whilst the formation of [ML] becomes complete. pK_a [ML] constants obtained by the two kinds of methods are in a good agreement.

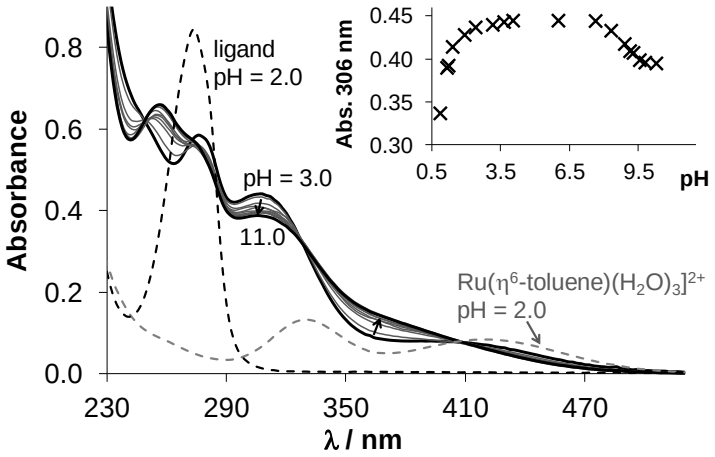

Figure 4. UV-vis absorption spectra recorded for the [Ru(η^6-toluene)$(H_2O)_3]^{2+}$ – 3-Me-picH (1:1) system in the presence of chloride ions in the pH range from 3 up to 11. The inset shows the absorbance changes at 306 nm at pH between 0.7 and 11. {c_{Ru} = *102 μM; T = 25 °C; I = 0.20 M (KCl); ℓ = 1.0 cm*}.

In addition ^{1}H NMR spectra were also recorded for the [Ru(η^6-toluene)$(H_2O)_3]^{2+}$ – pic system in the presence of 0.2 M chloride ions at a 1:1 metal-to-ligand ratio at various pH values using 4 h incubation time (Fig. 5). The spectra undoubtedly reveal that neither a free metal ion nor a ligand is present in the whole pH range studied (pH = 2 – 11.5), which means that the complex does not suffer from decomposition at 1 mM concentration due to its high stability. The aqua [ML(H_2O)] and the chlorinated [ML(Cl)] complexes were identified in the acidic pH range. An upfield shift of all peaks belonging to the [ML(H_2O)] complex is observed in the basic pH range due to the fast exchange process on the NMR time scale between the aquated and the mixed hydroxido [ML(OH)] species. In the meanwhile the intensity of the peaks

belonging to the [ML(Cl)] complex is decreased. Based on the integrals of the CH(6) toluene proton in the acidic pH range the [ML] complex is mainly chlorinated (~83% [ML(Cl)]). As the [ML(OH)] starts to be formed the three species are present together in the solution, and their equilibrium concentrations cannot be simply calculated due to the fast exchange process.

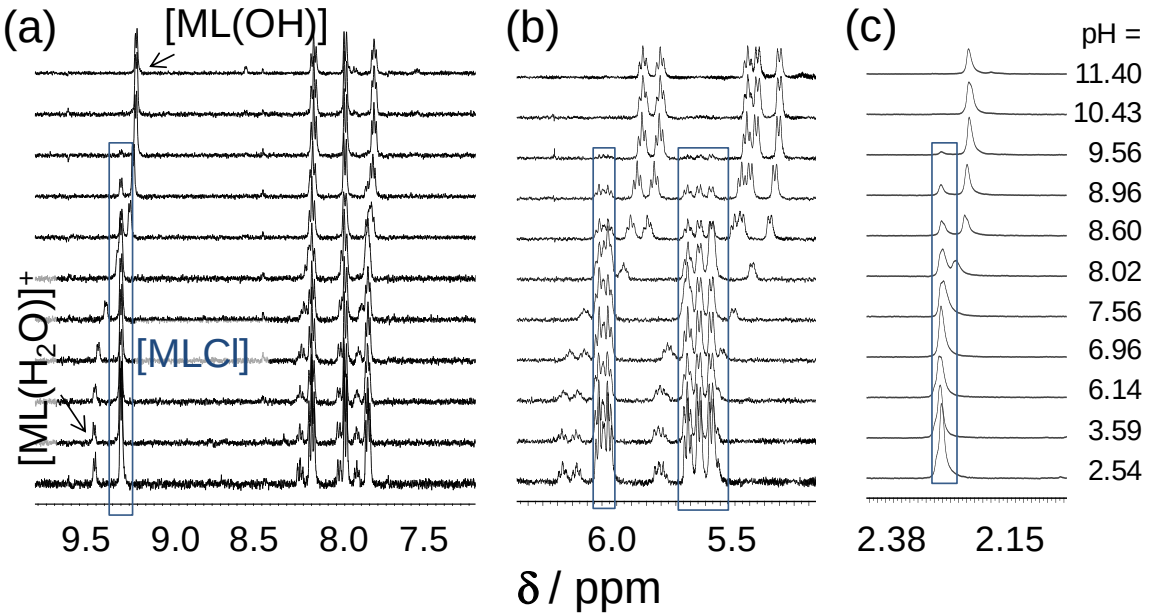

Figure 5. ^{1}H NMR spectra of [Ru(η^6-toluene)$(H_2O)_3$]$^{2+}$ – picH (1:1) system in aqueous solution in the presence of 0.2 M chloride ions at the indicated pH values in the regions of the ligand protons (a), the toluene CH protons (b) and the toluene CH_3 protons (c). {*c_{Ru} = 1 mM; T = 25 ˚C; I = 0.20 M (KCl); D_2O; pH = pD×0.93+0.40 [51]*}.

Therefore, the pK_a of the aqua [ML(H_2O)] was determined (pK_a = 7.87 ±0.09) based on the pH-dependent chemical shift (δ) values of [ML(H_2O)] and [ML(OH)] species. (Notably this value equals to the pK_a [ML] in the chloride-free medium.) Using this constant the ratio of the latter two species can be calculated at any chosen pH and then the actual concentrations of all the three complexes could be computed (Fig. 6). From the ratio of the summed concentration of [ML(Cl)] and [ML(H_2O)] (as [ML] species) and that of [ML(OH)] pK_a [ML] in the 0.2 M chloride-containing medium was calculated (Table 3) representing a good match to the data obtained by the other two methods.

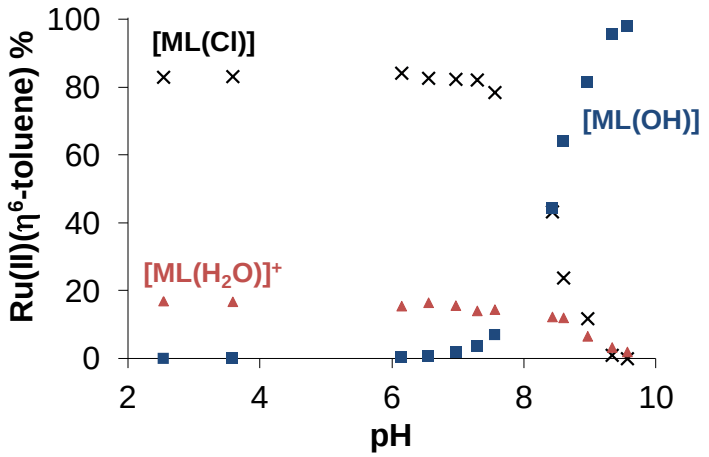

Figure 6. Distribution of Ru(η^6-toluene) in the [Ru(η^6-toluene)$(H_2O)_3$]$^{2+}$ – picH (1:1) system in the presence of 0.2 M chloride ions in the pH range from 2 up to 10 based on the ^{1}H NMR peak integrals for the CH(6) toluene proton of species identified based on Fig. 5. The ratio of the [ML$(H_2O)]^+$ and [ML(OH)] at a given pH is calculated using the pK_a [ML] of the aqua complex. {c_{Ru} *= 1 mM; T = 25 ˚C; I = 0.20 M (KCl)*}.

In order to compare the stability of the studied Ru(η^6-toluene) complexes of the different picolinates to each other pM* values were computed using the experimentally determined equilibrium constants (Table 3). pM is the negative logarithm of the equilibrium concentration of the unbound metal ion, and a higher pM value indicates a stronger metal ion binding ability of the ligand under given circumstances. Due to the hydrolysis of the Ru(η^6-toluene) fragment pM* was computed reflecting the unbound fraction of the metal ion where pM* = −log([M] + $[M_2(OH)_2]$ + $[M_2(OH)_3]$). These pM* values indicate the formation of relatively high stability complexes suggesting the following stability order at pH 7.4: **5** > **4** > **1** > **2** > **3**. *E.g.* decomposition of 1% and 20% are estimated for complexes **1** and **3** at 100 μM concentration, respectively. Based on the speciation data it can be concluded that the complexes are present mainly in their [ML] forms at pH 7.4, and they are only partly deprotonated ([ML(OH)] ~ 10%) in the 0.2 M chloride-containing medium.

The ratio of the chlorinated and aqua complexes ([ML(Cl)] and [ML(H_2O)]) can be characterized by the H_2O/Cl^- exchange constant, which was determined by UV-vis spectrophotometry using the same approach that we used in our previous works for analogous Rh(η^5-C_5Me_5) complexes [52,53]. Representative UV-vis spectra recorded at various chloride ion concentrations for the complex **1** and the measured and fitted absorbance values are shown in Fig. S9. Notably a lower H_2O/Cl^- exchange constant allows an easier replacement of Cl^- by water or by donor atoms of biomolecules. The log*K*' (H_2O/Cl^-) values (Table 3) obtained for

1-**5** reflect a moderate affinity towards chloride ions which is much lower compared to *e.g.* the analogous Rh(η^5-C_5Me_5) picolinate complexes [52,53]. The dependence of cytotoxicity on chloride ion affinity has been reported for several Ru(η^6-arene) complexes [54], however many other factors such as lipophilicity have a strong influence on the pharmacological activity. Therefore, distribution coefficients at pH 7.4 (log$D_{7.4}$) were determined for the complexes **1**-**5**, for the metal-free ligands and for the precursor [Ru(η^6-toluene)Cl(μ-Cl)]$_2$ at various chloride ion concentrations according to the chloride content of blood serum: ~100 mM, cell plasma: ~24 mM and cell nucleus: ~4 mM. The precursor, the ligands, the complexes **2**, **4** and **5** were found to be very hydrophilic at each studied chloride ion concentration (log$D_{7.4} < -2.5$). log$D_{7.4}$ values only for complexes **2** and **3** could be determined accurately by the applied *n*-octanol-water partitioning (Fig. 7), and they exhibit increasing lipophilicity with increasing chloride ion concentration, although even at 100 mM they are considered as fairly hydrophilic compounds. They have stronger hydrophilic character in the presence of less chloride ions since they are more aquated and the complex turns to be charged ([ML(Cl)] → [ML(H_2O]$^+$).

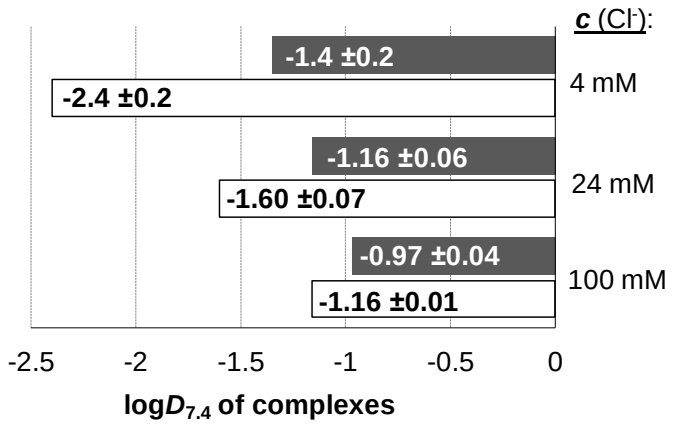

Figure 7. *n*-Octanol/water distribution coefficients at pH 7.4 (log$D_{7.4}$) for complexes **2** (white bars) and **3** (grey bars) at various chloride ion concentrations {*T = 25 °C, pH = 7.4 (20 mM phosphate buffer)*}

3.4. Cytotoxic and antiproliferative activity in human cancer cell lines

In order to evaluate the biological effects of complexes **1**-**5**, antiproliferative and cytotoxicity assays were applied in doxorubicin-sensitive (Colo 205) and multidrug resistant (Colo 320) human colonic adenocarcinoma cell lines. The resistance of Colo 320 cells is primarily mediated by the overexpression of ABCB1 (P-glycoprotein), a member of the ATP-binding cassette (ABC) transporter family, which pumps out xenobiotics from the cells. Cytotoxicity was measured in normal human embryonal lung fibroblast cells (MRC-5) as well. In addition the corresponding free ligands and the precursor [Ru(η^6-toluene)Cl(μ-Cl)]$_2$ were tested for

comparison. In case of the antiproliferative assay, a low cell number (6×10^3 cells/well) was chosen and the incubation period of the MTT assay was longer (72 h). Using these conditions information can be provided about the activity of the complexes to inhibit cell proliferation. In case of the cytotoxicity assay, a high cell number (2×10^4 cells/well) was used and the inhibition of cell growth was determined after 24 h by MTT assay. The latter assay is an important tool to investigate the toxicity of the complexes. In both assays cisplatin was used as a positive control. IC_{50} values are collected in Table S3. The ligands and the precursor did not show either cytotoxic or antiproliferative activities (IC_{50} >100 μM).

The complexes **1-5** did not possess any cytotoxic activity on the colon adenocarcinoma cell lines and on the normal MRC-5 human embryonic fibroblast cells. On the other hand the complexes **1** and **2** showed a moderate antiproliferative effect on the MDR Colo 320 colon adenocarcinoma cell line with IC_{50} values of 84.84 ± 4.79 and 79.19 ± 6.71 μM, respectively. Interestingly, these complexes had greater activity on the MDR cell line than on the sensitive Colo 205 cell line implying the selectivity of these complexes towards the MDR colon adenocarcinoma cell line.

Table 4. pK_a of the complexes $[ML(H_2O)]^+$ in the absence and in the presence of chloride ions at 0.2 M ionic strength, the Cl^-/H_2O exchange constants (log$K$' (H_2O/Cl^-) for the $[ML(H_2O)]^+ + Cl^- \rightleftharpoons [ML(Cl)] + H_2O$ equilibrium, estimated ratio of the chlorinated complex [ML(Cl)] at 4 and 100 mM chloride ion concentrations, and representative IC_{50} values measured in human cancer cells for the complexes of [Ru(η^6-toluene)(pic)Cl], [Ru(η^6-*p*-cymene)(pic)Cl], [Os(η^6-*p*-cymene)(pic)Cl] and [Rh(η^5-C_5Me_5)(pic)Cl].

	1	[**Ru**(η^6-*p*-cymene)(pic)Cl]	[**Os**(η^6-*p*-cymene)(pic)Cl]	[**Rh**(η^5-C_5Me_5)(pic)Cl]
pK_a (0 M Cl^-)	7.87	8.00 [b]	6.67 [d]	9.32 [e]
pK_a (0.2 M Cl^-)	8.53	8.90 [b]	n.d.	10.44 [e]
log$K$' (H_2O/Cl^-)	1.33	1.83 [b]	n.d.	2.20 [e]
rate of Cl^-/H_2O	fast	fast [b]	slower [d] $t_{1/2}$ ~ 12 min	fast [e]
[ML(Cl)] fraction				
c(Cl^-) = 4 mM	68%	87% [b]	100% [d]	94% [e]
c(Cl^-) = 100 mM	8%	22% [b]	28% [d]	36% [e]

IC_{50} (μM)	84.84±4.79 (Colo320) [a]	82 (HeLa) [c] 36 (FemX) [c]	17 (A549) [d] 4.5 (A2780) [d]	343 (A549) [e] 258 (CH1) [e]

[a] Antiproliferative activity; [b] Data taken from Ref. 23.; [c] Data taken from Ref. 27.; [d] Data taken from Ref. 29.; [e] Data taken from Ref. 52.

Among the half-sandwich organometallic complexes of picolinic acid reported in the literature [Os(η^6-*p*-cymene)(pic)Cl] has the highest cytotoxic effect [29], [Ru(η^6-*p*-cymene)(pic)Cl] is moderately cytotoxic [27], while compounds [Ru(η^6-toluene)(pic)Cl] (**1**) and [Rh(η^5-C_5Me_5)(pic)Cl] [52] possess much lower activity. In order to compare these complexes for getting insight their different biological activity some physico-chemical properties such as pK_a [ML], log$K$' (H_2O/Cl^-) are collected in Table 4. A low pK_a [ML] is generally considered to be unfavorable as the chance for the formation of the ternary mixed hydroxido [ML(OH)], that is believed to be less prone to interact with biomolecules [55], becomes higher at pH 7.4. In this context the Os(II) complex would be expected to be the least active. The effect of a strong chloride ion affinity (higher log$K$' (H_2O/Cl^-), thus higher fraction of the chlorinated complex) can be dual. If the affinity is high the complex can retain the original chlorido ligand coordinated more efficiently in the serum and the neutral [ML(Cl)] complex can go across the cell membrane easier via passive transport. Additionally the lipophilicity of the complex should be also optimal; however no log$D_{7.4}$ values are available for most of these complexes. On the other hand, after entering the cell, it is assumed that the lower intracellular chloride content can induce partial aquation of the complexes leading to the formation of the active aqua complex. When the chloride affinity is high, the replacement of Cl^- by water or donor atoms of proteins is aggravated. Besides these properties the reaction rate of the displacement reaction is also an important factor. Based on these parameters it seems that relatively slow kinetics of the Os(II) complex is advantageous. Whilst the strong hydrophilic character, fast Cl^-/water exchange process of the [Ru(η^6-toluene)(picolinate)Cl] studied in this work can be at least partly responsible due to the lack of their cytotoxicity.

*3.5. Interaction of complexes **1** and **2** with human serum albumin*

HSA is the most abundant plasma protein and serves as a transport vehicle for a wide variety of endogenous compounds and pharmaceuticals. Binding to HSA has a strong impact on the pharmacokinetic properties of drugs. In addition HSA-bound drugs are known to accumulate in solid tumors as a consequence of the enhanced permeability and retention effect, which can

be an operative way of selective tumor targeting [56]. This protein has various metal binding sites such as the N-terminal site, the reduced Cys34 residue, the multi-metal binding site and certain side chain donor atoms such as imidazole nitrogens of His are also able to coordinate to the metal ions [57,58]. On the other hand nonspecific binding pockets located in subdomains IIA and IIIA are willing to accommodate compounds of a wide variety [58]. In all diversified binding modes are possible for potential metallodrugs.

Interaction of complexes **1** and **2** representing moderate antiproliferative activity (see Section 3.4) towards HSA was studied by mainly ultrafiltration/UV-vis and spectrofluorometric methods. All measurements were performed at pH 7.4 at 25 ºC using a modified phosphate buffered saline (PBS') in which the concentration of the chloride ions corresponds to that of the human blood serum. First of all binding of **1** to HSA was monitored by ^{1}H NMR spectroscopy. Spectra were recorded for **1** in the absence or in the presence of the protein after a 24 h incubation period (Fig. S10). (This incubation time was chosen as the preliminary time-dependence studies showed that the reaction is relatively slow, depending on the conditions several hours are needed to reach the equilibrium state.) It was found that the signal of the toluene methyl group is shifted in the presence of HSA and no free ligand was detected. These observations strongly suggest the formation of ternary adducts with the protein without ligand cleavage. Then the direct interaction of complexes **1**, **2** and the $[Ru(\eta^6\text{-toluene})Cl(\mu\text{-}Cl)]_2$ precursor was followed by ultrafiltration. The unbound, low molecular mass (LMM) fractions after separation were analyzed by UV-vis quantification. Analysis of the recorded spectra confirmed that the complexes **1**, **2** are intact upon binding as we could not detect free ligand in the LMM fraction (Fig. S11). Comparing the spectra recorded after the separation to reference spectra the ratio of the bound compounds per HSA was calculated and plotted against the ratio of the total concentrations of the complexes and the protein (Fig. 8).

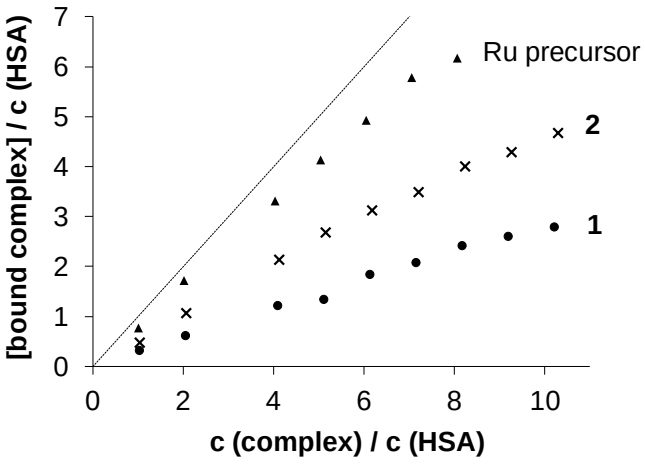

Figure 8. Ratio of the bound complexes (Ru precursor, **1** and **2**) and HSA plotted against the ratio of the total concentrations of the complexes and HSA calculated from the UV-vis spectra recorded for the LMM fractions of the ultrafiltered samples. {*Original sample composition: HSA: 40 μM; complexes: 0-400 μM; T = 25 ˚C; pH = 7.4 in PBS'*; *incubation time: 24 h*}.

These formation curves show the binding at multiple sites for the Ru precursor and for the complexes, although no saturation could be achieved up to the applied 10-fold complex excess. The binding of the precursor is almost quantitative, but realized at a lower level compared to the Rh(η^5-C_5Me_5) precursor [45]. The binding of **1** is somewhat weaker compared to **2**; however at least 3 or 5 binding sites are feasible for them, respectively.

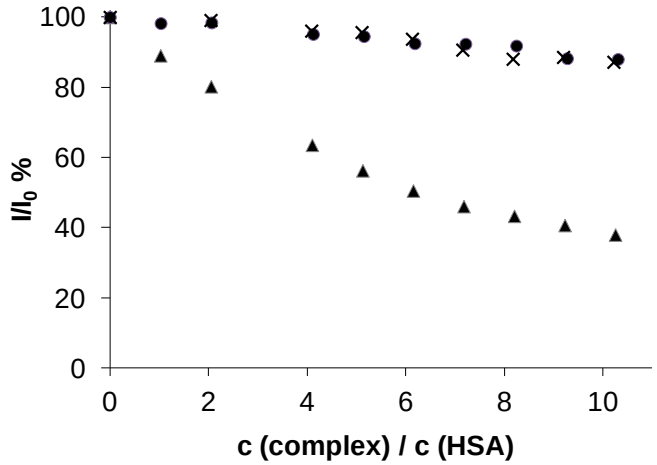

Figure 9. Changes of fluorescence emission intensities at 338 nm plotted against the complex-to-HSA ratios for 1 (●), 2 (×) and the Ru precursor (▲) using 295 nm excitation and 340 nm emission wavelengths. {c_{HSA} *= 1 μM; complexes: 0-10 μM; T = 25 ˚C; pH = 7.4 in PBS'*; *incubation time: 24 h*}.

In order to obtain preliminary information about the binding sites the interaction of **1**, **2** and the Ru(II) precursor were monitored by fluorometry. HSA contains a single Trp (214) residue near site I (at subdomains IIA) that is responsible for the majority of the intrinsic fluorescence of the protein. Upon excitation at 295 nm its emission can be attenuated by a binding event close to Trp214 [58,59]. It is worth mentioning that coordination of protein side chains such as histidine nitrogens (*e.g.* His242) [59] located nearby this site to the ruthenium complexes by the substitution of the chlorido/aqua ligand at the third coordination site is very feasible. Addition of the Ru(II) compounds to HSA quenches the Trp214 fluorescence emission (Fig. 9) indicating that the conformation of the hydrophobic binding pocket is significantly affected upon their binding. Based on the emission intensity changes quenching constants were computed. Log$K_{Q'}$ values of 5.25 ±0.01, 4.16 ±0.01 and 4.18 ±0.01 were obtained for the Ru precursor, **1** and **2**, respectively. These values reflect fairly strong binding of the precursor, and

a moderate and similar binding of **1** and **2** at this particular site of HSA. As more than one binding sites are suggested on the basis of the ultrafiltration measurements, the complexes **1** and **2** (as well as the precursor) should be bound on other sites beside site I as well, such as the more accessible surface donors. Among the side chain donors His, Met and Cys residues are suggested to be responsible to coordinate to Ru complexes [60,61]. The prominent role of His was pointed out in the case of Rh(η^5-C_5Me_5) complexes in our former work [45]. Therefore interaction of **1** and the precursor with 1-methylimidazole (N-MeIm), a monodentate model compound of His, was screened by ^{1}H NMR spectroscopy. It was found that 95% the Ru(II) precursor is bound to N-MeIm at 1:1 ratio (Fig. S12), while 100% of the analogous [Rh(η^5-C_5Me_5)Cl(μ-Cl)]$_2$ precursor is bound under the same condition [45]. In the case of complex **1** the original picolinate ligand was not replaced by the model compound but formation of ternary [Ru(η^6-toluene)(pic)(N-MeIm)] complex of significant fraction (**1**: 85%) was observed (Fig. S13). This observation confirms the feasible coordination of the imidazole nitrogen of His at the third coordination site of the studied picolinate complexes.

4. Conclusions

Metal complexes of 2-picolinic acid and its 3-methyl, 5-bromo, 4-carboxylic, 5-carboxylic derivatives formed with Ru(η^6-toluene) organometallic fragment were synthesized and characterized in solid phase and in solution. The structures of four complexes were also determined by single-crystal X-ray diffraction showing a pseudo-octahedral "pianostool" geometry, and the deprotonated picolinates bind in a bidentate mode via (N,O) donor atoms and the coordination sphere is completed by a chlorido ligand. Complex formation equilibrium processes were studied in aqueous solution by the combined use of UV-visible spectrophotometry, pH-potentiometry and ^{1}H NMR spectroscopy in the presence of chloride ions in addition to the characterization of the proton dissociation equilibria of the ligands. The complex formation reached a significant extent already at pH 0.7 representing prominently high stability and was found to be relatively slow (*ca.* 35 min); while deprotonation of the complex and water/chloride exchange processes took place fast. By means of these methods we could demonstrate exclusive formation of mono complexes such as [Ru(η^6-toluene)(L)(Z)] (L: completely deprotonated ligand; Z = H_2O/Cl^-) and [Ru(η^6-toluene)(L)(OH)] in solution. Moderate pK_a values (8.3-8.7) were obtained reflecting the formation of *ca.* 10% mixed hydroxido species at pH 7.4 in the presence of 0.2 M KCl. The chloride ion affinity of the complexes was characterized by moderate H_2O/Cl^- co-ligand exchange equilibrium constants

(log*K*' H_2O/Cl^- = 1.1-1.5) which are lower than those of the analogous Ru(η^6-*p*-cymene) and Rh(η^5-C_5Me_5) compounds.

All the studied metal complexes exhibit a rather hydrophilic character at 100 mM chloride concentration and become even more hydrophilic at lower chloride content. The studied complexes were not cytotoxic against colon adenocarcinoma cell lines and normal MRC-5 human embryonic fibroblast cells. However, the complexes formed with 2-picolinic acid (**1**) and its 3-methyl derivative (**2**) represented a moderate antiproliferative effect (IC_{50} = 84.84, 79.19 μM) on the multidrug resistant Colo 320 colon adenocarcinoma cell line revealing considerable MDR selectivity. Interaction of complexes **1** and **2** with the blood transport protein HSA was investigated by ultrafiltration and fluorometry. The binding is relatively slow and no ligand cleavage was observed, thus formation of ternary adducts with the protein via coordination bonds at several binding sites (at least 3-5) is suggested. Complex **1** represents a somewhat weaker overall binding compared to **2**, while their binding at site I is fairly similar based on the Trp(214) quenching studies. 1-methylimidazole binds efficiently to these complexes at the third coordination site suggesting the probable binding of imidazole nitrogens of the protein with non-dissociative characteristics.

Abbreviations:

5-Br-picH	5-bromo-2-pyridinecarboxylic acid
cisplatin	*cis*-[$Pt(NH_3)_2(Cl)_2$]
$D_{7.4}$	distribution coefficients at physiological pH
2,4-dipicH_2	2,4-pyridinedicarboxylic acid
2,5-dipicH_2	2,5-pyridinedicarboxylic acid
DSS	4,4-dimethyl-4-silapentane-1-sulfonic acid
EMEM	Eagle's Minimal Essential Medium
HSA	human serum albumin
MDR	multidrug resistance
3-Me-picH	3-methylpyridine-2-carboxylic acid
MTT	3-(4,5-dimethyl-2-thiazolyl)-2,5-diphenyl-2H-tetrazolium bromide
NKP-1339	sodium *trans*-[Ru(III)$Cl_4(Ind)_2$], Ind = indazole; IT-139
N-MeIm	1-methylimidazole
PBS'	modified phosphate-buffered saline
picH	pyridine-2-carboxylic acid, 2-picolinic acid
UV-vis	UV-visible

Acknowledgements

This work was supported by National Research, Development and Innovation Office-NKFIH through projects GINOP-2.3.2-15-2016-00038, OTKA FK 124240, OTKA K 115762, the New National Excellence Program UNKP-17-4-III-SZTE-13 (E.A.E.), the J. Bolyai Research Scholarship of the Hungarian Academy of Sciences (N.V.M.) and Ministry of Education, Science and Technological development – Republic of Serbia (MPNTR 172035 and MPNTR postdoctoral grant (J. M. P.)).

Appendix A. Supplementary data

Supplementary data associated with this article can be found online at…

References

[1] G.N. Kaluderovic, R. Paschke, Curr. Med. Chem. 18 (2011) 4738–4752.

[2] M.A. Jakupec, M. Galanski, V.B. Arion, C.G. Hartinger, B.K. Keppler, Dalton Trans. (2008) 183–194.

[3] L. Zeng, P. Gupta, Y. Chen, E. Wang, L. Ji, H. Chao, Z-S. Chen, Chem. Soc. Rev. (2017) Advance Article, doi: 10.1039/C7CS00195A

[4] E. Alessio, Eur. J. Inorg. Chem. 2017 (2017) 1549–1560.

[5] R. Trondl, P. Heffeter, C.R. Kowol, M.A. Jakupec, W. Bergerbd, B.K. Keppler, Chem. Sci. 5 (2014) 2925–2932.

[6] H.A. Burris, S. Bakewell, J. Bendell, J. Infante, S. Jones, D. Spigel, G.J. Weiss, R.K. Ramanathan, A. Ogden, D. Von Hoff, ESMO Open, 1 (2017) e000154.

[7] Y. Jung, S.J. Lippard, Chem. Rev. 107 (2007) 1387–1407.

[8] B. Schoenhacker-Alte, T. Mohr, C. Pirker, K. Kryeziu, P.S. Kuhn, A. Buck, T. Hofmann, C. Gerner, G. Hermann, G. Koellensperger, B.K. Keppler, W. Berger, P. Heffeter, Cancer Lett. 404 (2017) 79–88.

[9] https://clinicaltrials.gov/ct2/show/NCT03053635?term=tld-1433&recrs=a&rank=1. Accessed on 13/09/2017

[10] B.S. Murray, M.V. Babak, C.G. Hartinger, P.J. Dyson, Coord. Chem. Rev. 306 (2016) 86–114.

[11] A. Weiss, R. H. Berndsen, M. Dubois, C. Müller, R. Schibli, A. W. Griffioen, P. J. Dyson and P. Nowak-Sliwinska, Chem. Sci. 5 (2014) 4742–4748.

[12] R.E. Morris, R.E. Aird, P.D. Murdoch, H.M. Chen, J. Cummings, N.D. Hughes, S. Parsons, A. Parkin, G. Boyd, D.I. Jodrell, P.J. Sadler, J. Med. Chem. 44 (2001) 3616–3621.

[13] R.L. Hayward, Q.C. Schornagel, R. Tente, J.C. Macpherson, R.E. Aird, S. Guichard, A. Habtemariam, P. Sadler, D.I. Jodrell, Cancer Chemother. Pharmacol. 55 (2005) 577–583.

[14] W.H. Ang, A. Casini, G. Sava, P.J. Dyson, J. Org. Chem. 696 (2011) 989–998.

[15] B. Therrien, Coord. Chem. Rev. 253 (2009) 493–519.

[16] S.H. van Rijt, P.J. Sadler, Drug Discov. Today 14 (2009) 1089–1097.

[17] A. Merlino, Coord. Chem. Rev. 326 (2016) 111–134.

[18] L. Bíró, E. Farkas, P. Buglyó, Dalton Trans. 39 (2010) 10272–10278.

[19] L. Bíró, E. Balogh, P. Buglyó, J. Organomet. Chem. 734 (2013) 61–68.

[20] D. Hüse, L. Bíró, J. Patalenszki, A.C. Bényei, P. Buglyó, Eur. J. Inorg. Chem. 2014 (2014) 5204–5216.

[21] Z. Bihari, Z. Nagy, P. Buglyó, J. Organomet. Chem. 782 (2015) 82–88.

[22] É.A. Enyedy, É. Sija, T. Jakusch, C.G. Hartinger, W. Kandioller, B.K. Keppler, T. Kiss, J Inorg. Biochem. 127 (2013) 161–168.

[23] É. Sija, C.G. Hartinger, B.K. Keppler, T. Kiss, É.A. Enyedy, Polyhedron 67 (2014) 51–58.

[24] O. Dömötör, V.F.S. Pape, N.V. Nagy, G. Szakács, E.A. Enyedy, Dalton Trans. 46 (2017) 4382–4396.

[25] N. Gligorijevic, S. Arandelovic, L. Filipovic, K. Jakovljevic, R. Jankovic, S. Grguric-Sipka, I. Ivanovic, S. Radulovic, Z.Lj, Tesic, J. Inorg. Biochem. 108 (2012) 53–61.

[26] S. Grguric-Šipka, I. Ivanovic, G. Rakic, N. Todorovic, N. Gligorijevic, S. Radulovic, V.B. Arion, B.K. Keppler, Eur. J. Med. Chem. 45 (2010) 1051–1058.

[27] I. Ivanovic, S. Grguric-Šipka, N. Gligorijevic, S. Radulovic, A. Roller, Z.Lj. Tešic, B.K. Keppler, J. Serb. Chem. Soc. 76 (2011) 53–61.

[28] I. Ivanovic, K.K. Jovanovic, N. Gligorijevic, S. Radulovic, V.B. Arion, K.S.A.M. Sheweshein, Z.Lj. Tesic, S. Grguric-Sipka, J. Organomet. Chem. 749 (2014) 343–349.

[29] A.F.A. Peacock, S. Parsons, P.J. Sadler, J. Am. Chem. Soc. 129 (2007), 3348–3357.

[30] P. Gans, A. Sabatini, A. Vacca, Talanta 43 (1996) 1739–1753.

[31] R.A. Zelonka, M.C. Baird, Can. J. Chem. 50 (1972) 3063–3072.

[32] G.H. Beaven, S. Chen, A. D'Albis, W.B. Gratzer, Eur. J. Biochem. 42 (1974) 539–546.

[33] T.Higashi, Numerical Absorption Correction, NUMABS (2002)

[34] CrystalClear SM 1.4.0 Rigaku/MSC Inc. (2008)

[35] M.C. Burla, R. Caliandro, B. Carrozzini, G.L. Cascarano, C. Cuocci, C. Giacovazzo, M. Mallamo, A. Mazzone, G. Polidori, J. Appl. Crystallogr. 48 (2015) 306–309.

[36] SHELXL-2013 Program for Crystal Structure Solution, University of Göttingen, Germany (2013)

[37] L.J. Farrugia, J. Appl. Crystallogr. 45 (2012) 849–854.

[38] A.L. Spek, J. Appl. Crystallogr. 36 (2003) 7–13.

[39] C.F. Macrae, P.R. Edgington, P. McCabe, E. Pidcock, G.P. Shields, R. Taylor, M. Towler, J. van De Streek, J. Appl. Crystallogr. 39 (2006) 453–457.

[40] S.P. Westrip, J. Appl. Crystallogr. 43 (2010) 920–925.

[41] H.M. Irving, M.G. Miles, L.D. Pettit, Anal. Chim. Acta 38 (1967) 475–488.

[42] SCQuery, The IUPAC Stability Constants Database, Academic Software (Version 5.5), R. Soc. Chem., 1993–2005.

[43] L. Bíró, A.J. Godó, Z. Bihari, E. Garribba, P. Buglyó, Eur. J. Inorg. Chem. 2013 (2013) 3090–3100.

[44] L. Zékány, I. Nagypál, in: Computational Methods for the Determination of Stability Constants (Ed.: D.L. Leggett), Plenum Press, New York, 1985, pp. 291–353

[45] É.A. Enyedy, J.P. Mészáros, O. Dömötör, C.M. Hackl, A. Roller, B.K. Keppler, W. Kandioller, J. Inorg. Biochem. 152 (2015) 93–103.

[46] O. Dömötör, C.G. Hartinger, A.K. Bytzek, T. Kiss, B.K. Keppler, E.A. Enyedy, J. Biol. Inorg. Chem. 18 (2013) 9–17.

[47] R.S. Cahn, C. Ingold, V. Prelog, Angew. Chem., Int. Ed. Engl. 5 (1966) 385–415.

[48] K.D. Camm, A. El-Sokkary, A.L. Gott, P.G. Stockley, T. Belyaeva, P.C. McGowan, Dalton Trans. (2009) 10914–10925.

[49] W.S. Sheldrick, S. Heeb, Inorg. Chim. Acta 168 (1990) 93–100.

[50] É.A. Enyedy, D. Hollender, T. Kiss, J. Pharm. Biomed. Anal. 54 (2011) 1073–1081.

[51] K. Ősz, G. Lente, C. Kállay, J. Phys. Chem. B 109 (2005) 1039–1047.

[52] É.A. Enyedy, O. Dömötör, C.M. Hackl, A. Roller, M.S. Novak, M.A. Jakupec, B.K. Keppler, W. Kandioller, J. Coord. Chem. 68 (2015) 1583–1601.

[53] O. Dömötör, C.M. Hackl, K. Bali, A. Roller, M. Hejl, M.A. Jakupec, B.K. Keppler, W. Kandioller, E.A. Enyedy, J. Organomet. Chem. 846 (2017) 287–295.

[54] Y.K. Yan, M. Melchart, A. Habtemariam, P.J. Sadler, Chem. Commun. (2005) 4764–4776.

[55] F. Wang, H. Chen, S. Parsons, I.D.H. Oswald, J.E. Davidson, P.J. Sadler, Chem. Eur. J. 9 (2003) 5810–5820.

[56] F. Kratz, J. Control. Release 132 (2008) 171–183.

[57] W. Bal, M. Sokołowska, E. Kurowska, P. Faller, Biochim. Biophys. Acta 1830 (2013) 5444–5455.

[58] G. Fanali, A. Masi, V. Trezza, M. Marino, M. Fasano, P. Ascenzi, Mol. Asp. Med. 33 (2012) 209–290.

[59] T. Peters, All About Albumin: Biochemistry, Genetics and Medical Applications, Academic Press, San Diego, 1996

[60] W. Hu, Q. Luo, X. Ma, K. Wu, J. Liu, Y. Chen, S. Xiong, J. Wang, P.J. Sadler, F. Wang, Chem. Eur. J. 15 (2009) 6586–6594.